Influence of hydrogen environment on fatigue crack growth in forged Ti-6Al-4V: fractographic analysis

2013 IOP Conf. Ser.: Mater. Sci. Eng. 48 012010

(http://iopscience.iop.org/1757-899X/48/1/012010)

Influence of hydrogen environment on fatigue crack growth in forged Ti-6Al-4V: fractographic analysis

R Gaddam[1], R Pederson[1], M Hörnqvist[2], M-L Antti[1]
[1]Division of Materials Science, Luleå University of Technology, 97187 Luleå, Sweden

[2]Department of Applied Physics, Chalmers University of Technology, 41296 Göteborg, Sweden

E-mail: raghuveer.gaddam@ltu.se

Abstract. The influence of high-pressure gaseous hydrogen environment (15 MPa) on the fatigue crack growth in forged Ti-6A1-4V at room temperature is investigated. It is observed that the fatigue crack growth (FCG) rate is fluctuating at $20 \leq \Delta K \leq 26$ MPa√m, and increase drastically at $\Delta K > 26$ MPa√m in hydrogen environment. The effect of hydrogen on the FCG rate is dependent on the stress intensity level (ΔK). Detailed fractographic analysis of the fracture surfaces is performed at different ΔK using field emission scanning electron microscope (FE-SEM). The differences in appearance of fracture surfaces in air and hydrogen are discussed.

1. Introduction

Titanium and its alloys are widely used in aerospace industry owing to their combination of high specific strength (i.e. strength/density), good fatigue strength and excellent corrosion resistance [1-2]. Among the many, Ti-6Al-4V (referred hereafter as Ti-64) is the principal alloy that is used in aeroengines up to 300°C [2]. Despite its exceptional properties, it has very limited usage in space applications. One of the major concerns is its incompatibility with hydrogen [3]; which is primarily used as fuel or coolant in rocket engines. Previous studies [4-9] have shown that presence of hydrogen in an environment (i.e. gaseous hydrogen) degraded mechanical properties such as ductility, fracture toughness and fatigue strength at ambient temperature.

Ti-64 is an aerospace alloy; the components made of this alloy are subjected to cyclic loads in service where the fatigue properties are of particular importance. If the alloy is intended for use in space applications, increased understanding of the effect of hydrogen on fatigue properties is required. The aim of the present work was to perform a detailed fractographic analysis to understand the effect of hydrogen environment (15 MPa) on fatigue crack growth resistance of forged Ti-64 at room temperature.

2. Materials and methods

2.1. Materials and environment

The material investigated is a Ti-64 alloy in forged condition, which has a bi-modal microstructure i.e. consisting of primary α and transformed β grains (see figure 1(a)). Transformed β is represented by α/β structure containing α colonies and α laths (figure 1(b)). Table 1 shows the quantitative information of these microstructural features. The environments used were ambient air and high-pressure gaseous hydrogen (≈ 99.995% purity), where the desired pressure (15 MPa) was obtained by pressurizing the test chamber prior to testing.

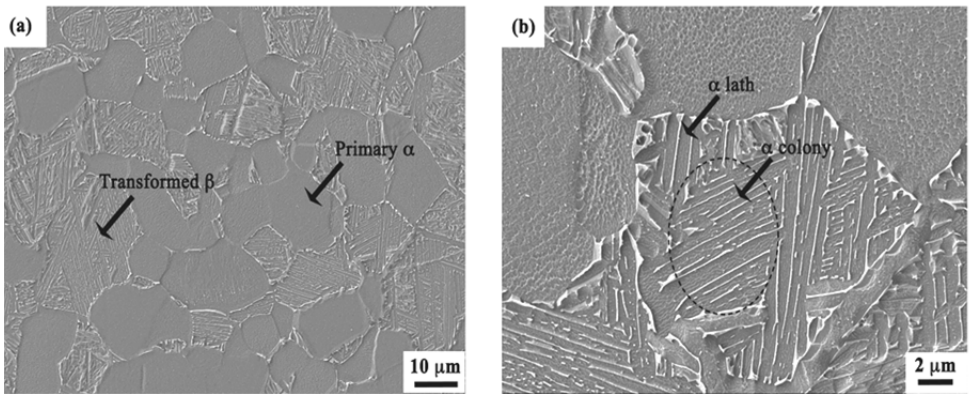

Figure 1. (a) Scanning electron micrographs of forged Ti-64 revealing the bi-modal microstructure with primary α and transformed β grains, (b) Magnified image of transformed β in (a) showing the α/ β structure. Grey area represents α phase and white shows β phase.

Table 1. Measurements of microstructural features in forged Ti-64 alloy.

Volume fraction of primary α (%)	Volume fraction of transformed β (%)	Size of primary α (μm)	Size of transformed β (μm)	Size of α colony (μm)	Alpha lath thickness (μm)
42.5	57.5	15 ± 3.87	18 ± 5.68	10 ± 2.68	0.52 ± 0.15

2.2. Fatigue crack growth testing

Fatigue crack growth (FCG) testing was conducted using a servohydraulic test rig on one sample each in ambient air and hydrogen environment at room temperature. The test specimens used were Kb-type, which have rectangular cross sections of 4.3 x 10.2 mm in the gauge section (dotted box in figure 2(a)). An initial starter notch of nominal depth of 0.1 mm and total width of 0.2 mm was introduced using electric discharge machining. The specimens along with the grips were enclosed in the autoclave as shown in figure 2(b), and the loads measured were corrected for internal autoclave pressure and piston seal friction. The specimens were pre-cracked under fatigue loading in air at room temperature, at a frequency of 10 Hz with a stress ratio $R = \sigma_{min}/\sigma_{max} = 0$, to obtain an initial crack length of ~ 0.5 mm. After pre-cracking, FCG testing was carried out by loading the specimens uniaxially with $R = 0$ and a frequency of 0.5 Hz, with triangular waveform by using the applicable parts of ASTM E647-08 [10] and ASTM E740-03 [11]. In these tests, the total crack lengths were measured by the direct current potential drop (PD) technique according to ASTM E 647 using an experimentally obtained calibration function to relate the PD signal to crack length. The tests were interrupted at an approximate total crack length of 2.6 mm. After the testing, the specimen tested in hydrogen environment was heat treated at about 150°C to mark the final crack front on the fracture surface.

The stress intensity factor range, ΔK, was calculated according to ASTM E740 as:

$$\Delta K = f * \Delta\sigma * \sqrt{(\pi a)} \quad (1)$$

where $\Delta\sigma$ is the applied stress range, a is the crack length and ı is a geometric factor based on specimen and crack geometry. Here, ΔK was calculated for the deepest point of the crack assuming a

semi-circular shape, which was verified from the fracture surfaces. As the applied stress range was different for the tests in air and hydrogen (450 and 530 MPa, respectively), equation (1) was also used to correlate the crack lengths (ı) between the tests, in order to compare fractographic results obtained at the same value of ΔK.

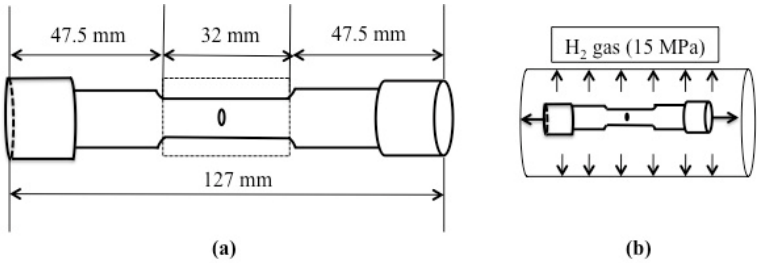

Figure 2. (a) Schematic diagram showing the dimensions of the Kb type specimen used in testing and (b) schematic illustration of testing in 15 MPa H_2 gas in closed autoclave.

2.3. Fractography

Fractographic analysis of fracture surfaces after the FCG tests were conducted using a field emission gun scanning electron microscope (FE-SEM) from Carl Zeiss (MERLIN® FE-SEM). The analysis were performed using secondary electrons with an accelerating voltage of 3 kV and probe current of 1 nA. During fractographic observations, attention was paid on specific regions showing distinct changes in the fracture surface features along the crack propagation direction.

3. Results and discussion

3.1. Fatigue crack growth (FCG) rate

FCG rate curve of forged Ti-64 in ambient air and gaseous hydrogen environment is shown in figure 3(a). It is expressed by showing a relation between fatigue crack growth rate (da/dN in mm/cycle) and stress intensity factor range (ΔK in MPa$\sqrt{m}$). Figure 3(b) shows the ratio of FCG rate change as a function of stress intensity. It was determined at various stress-intensity factor ranges (ΔK) by dividing the crack growth rate in hydrogen $(da/dN)_{hydrogen}$ by that obtained in air $(da/dN)_{air}$.

The results from FCG testing in air and hydrogen environment can be described by dividing the FCG rate curve into three distinct regions (see figure 3(b)). These regions are also reflected in the changes seen on the macroscopic fracture surface (see figure 4(b)). In the first region, denoted FCG-1 ($\Delta K \leq 20$ MPa$\sqrt{m}$, $a \leq 1.2$ mm), the da/dN ratio values are found to be nearly 1. It means that the FCG rate in hydrogen environment remains unaffected at low stress intensity range, and showing a stable crack growth similar to the one found in air. In the second region, denoted FCG-2 ($20 \leq \Delta K \leq 26$ MPa$\sqrt{m}$, $1.2 \leq a \leq 1.5$ mm), the da/dN ratio values are lower, on average, which shows that the FCG rate in hydrogen environment is lower than in air at intermediate stress intensity range. It is also observed that there are fluctuations in the da/dN values up to $\Delta K \approx 26$ MPa$\sqrt{m}$. These fluctuations show that crack growth is not stable or crack is temporarily arrested in hydrogen environment. Finally, in the third region, denoted as FCG-3 ($\Delta K > 26$ MPa$\sqrt{m}$, $a \geq 1.5$ mm), the da/dN ratio values drastically increase to 4.5. It means that the FCG rate is increased in gaseous hydrogen environment compared to air at high stress intensity ranges.

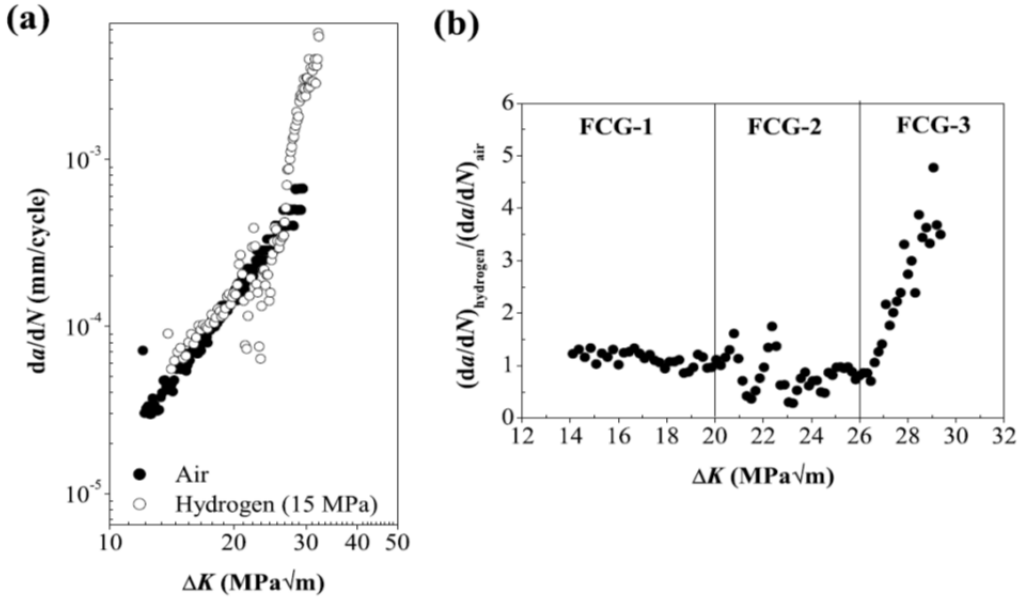

Figure 3. (a) Fatigue crack growth (FCG) rate of forged Ti-64 in air and hydrogen environment expressed in terms of da/dN versus ΔK, (b) Fatigue crack growth rate ratio curve showing the degree of crack growth enhancement caused by the hydrogen environment.

From the test results, it can be said that the FCG rate is significantly increased in hydrogen environment at high stress intensity range and the degree of increment is dependent on the stress intensity range (ΔK). There is a critical stress intensity value ($\Delta K^* \approx 20$ MPa√m), above which the influence of hydrogen on the fatigue crack growth is clearly noticeable. Observations in the change of FCG rate in hydrogen environment are reported elsewhere for Ti-64 alloy [8, 9, 12, 13]. Pittinato et al. [8, 9] showed that FCG rate increased in hydrogen environment compared to tests in helium gas when tested at room temperature to -17°C and showed that the FCG rate is dependent on the stress intensity range. However, Evans et al. [12] and Ding et al. [13] found that the FCG rate was lower in hydrogen environment than in air at room temperature. From these studies, it can be said that the influence of hydrogen environment on the FCG rate at room temperature might be dependent on several parameters such as test conditions (cyclic frequency, applied load, stress ratio), hydrogen pressure [14] and microstructure [6].

3.2. Fractography

Figure 4(a) and figure 4(b) show an overview of the fracture surfaces observed on the samples tested in air and hydrogen environment. In addition, specific regions of interest are marked that describe the influence of hydrogen on FCG rate as shown in figure 3(b). The fracture surface in air was denoted as FCG-1. However, in hydrogen environment, the fracture surfaces are classified into three distinct regions FCG-1, FCG-2 and FCG-3 as mentioned in section 3.1 (see figure 4(d-f)). Figure 5, figure 6 and figure 7 show the high-resolution micrographs of representative fracture surfaces observed in these regions. Table 2 provides a brief summary of the fracture surface features. Analysis of the entire fracture surfaces in air and hydrogen environment at $\Delta K \leq 20$ MPa√m (i.e. FCG-1 region) showed ductile features (see figure 4(c), figure 4(d)). Here, the fracture surfaces mainly consist of fatigue striations perpendicular to the fatigue crack propagation direction, which vary in size with ΔK (see figure 5(a) and figure 5(b)). At $20 \leq \Delta K \leq 26$ MPa√m (i.e. FCG-2 region), the fracture surface in

hydrogen environment consists of a mixture of flat areas containing features which look like crack arrest marks (see figure 6(a) and figure 6(e-f)), secondary cracks (see figure 4(e) and figure 6(a-f)), and fatigue striations similar to the one observed in FCG-1 (see figure 6(d)). The variation in fracture surface appearance at these intermediate ΔK values agrees with the fluctuations observed in da/dN ratio values (see figure 3(b)). Finally, at $\Delta K > 26$ MPa$\sqrt{m}$, the fracture surface in air consists of fatigue striations (see figure 7(a)). However, in hydrogen environment (i.e. in FCG-3 region), the fracture surface has a substantial increase of secondary cracks (see figure 4(f), figure 7(b)), and looks brittle.

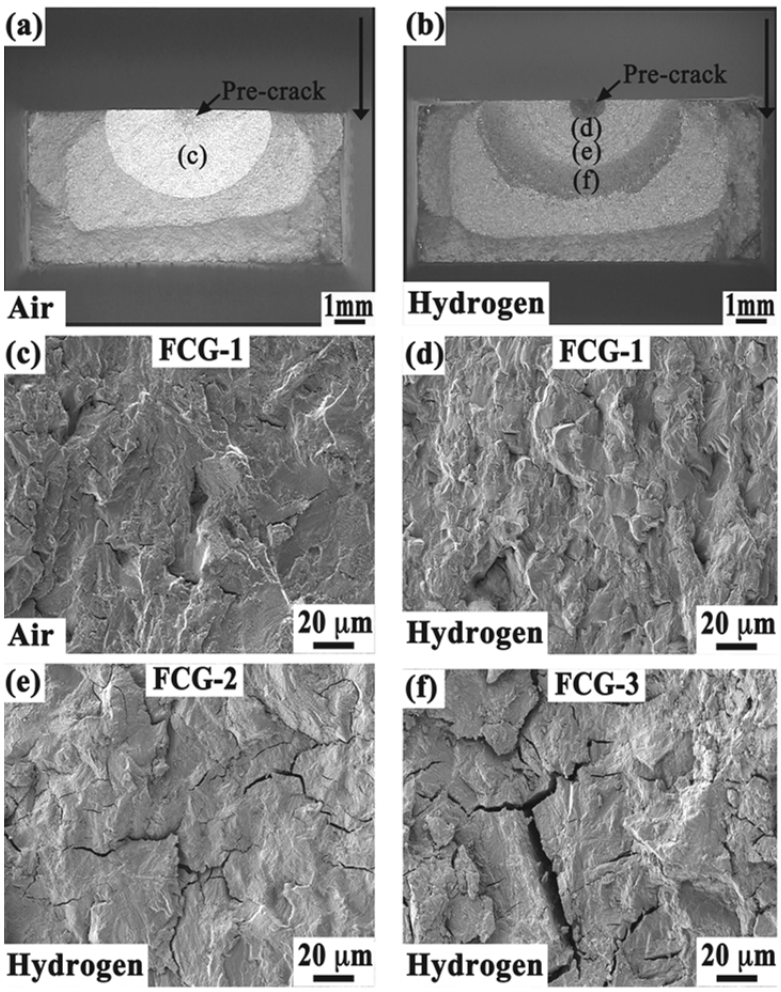

Figure 4. Micrographs showing the macroscopic fracture surfaces in (a) air and (b) hydrogen. Magnified images (c,d) show the similar appearance at low ΔK values, (e, f) show the presence of secondary cracks in hydrogen environment beyond the critical ΔK^* values. Arrows indicates the direction of crack propagation.

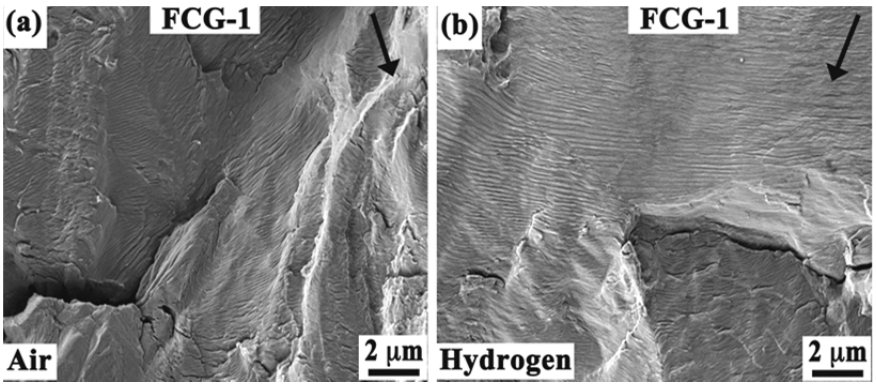

Figure 5. Representative micrographs of fatigue fracture surfaces in FCG-1 region ($\Delta K \leq 20$ MPa√m) of samples tested in air (a) and hydrogen (b) showing the presence of striations. Arrows indicate the crack propagation direction.

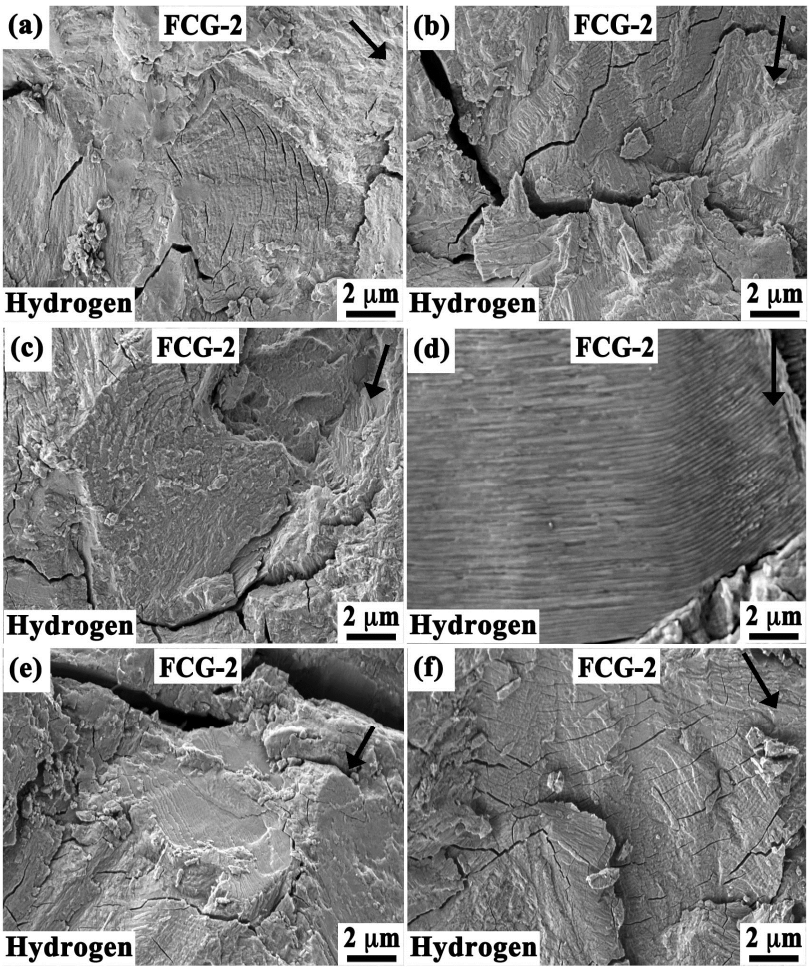

Figure 6. Representative micrographs of fatigue fracture surfaces in hydrogen environment along the FCG-2 region: (a-c) $\Delta K \approx 22$ MPa√m, (d) $\Delta K \approx 23$ MPa√m, (e) $\Delta K \approx 24$ MPa√m and (f) $\Delta K \approx 26$ MPa√m. Arrows indicate the crack propagation direction.

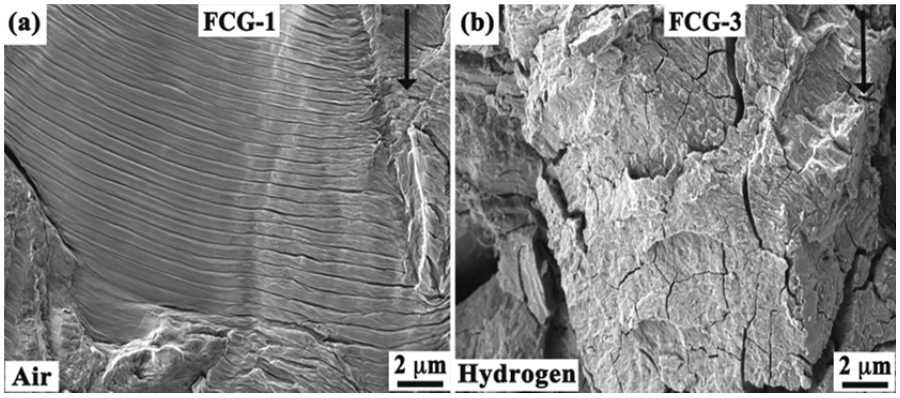

Figure 7. Representative micrographs of fatigue fracture surfaces at $\Delta K \approx 28$ MPa√m in (a) air and (b) hydrogen environment. Arrows indicate the crack propagation direction.

Table 2. Summary of the fatigue fracture surface appearance in the different FCG regions.

Region	ΔK (MPa√m)	Environment	
		Air	Hydrogen
FCG-1	≤ 20	Mostly striations	Mostly striations
FCG-2	20 – 26	Mostly striations	Mix of striated areas and flat regions. Decreasing amount of striated areas and increasing density of secondary cracks and crack arrest marks with increasing ΔK
FCG-3	> 26	Mostly striations	No striations, high density of secondary cracks

The observations made on fracture surfaces at different regions in hydrogen environment are consistent with the FCG behaviour described in section 3.1. In FCG-1 region (i.e. at lower ΔK), fracture surfaces mainly consist of fatigue striations; presumably the stress is too low for accumulation of hydrogen ahead of the crack tip. Instead the crack growth is dominated by the same mechanisms as in air. However, in FCG-2 region (i.e. at intermediate ΔK), the effect of hydrogen is clearly noted. Here, fracture surfaces mostly consist of secondary cracks that might have occurred due to an increase of stresses locally at the crack tip in presence of hydrogen and resulting in crack branching, which may lower the da/dN values [15]. In addition, the fracture surfaces also consist of relatively flat areas with feature resembling crack arrest marks that might be the result of a stress induced hydride formation and cracking as reported by Nelson et. al. [6, 7]. It is presumed that there could be enough time available for hydrogen to accumulate in front of the crack tip and precipitate as brittle hydrides at these intermediate stress intensity ranges, similar to what was observed by Shih et. al. [16] in a Ti-4Al alloy. Therefore, it seems that the fluctuation in FCG rate in hydrogen at these stress intensity levels could be attributed to the competing effects due to crack branching and brittle fracture of hydrides. Finally in FCG-3 region (i.e. at higher ΔK), the fracture surface consists of rough surface morphology with higher density of secondary cracks and a brittle appearance. At these higher stress intensities, it seems that the crack growth by fracture of hydrides is not possible, as there is no sufficient time for hydride formation. Instead the hydrogen diffused would accumulate at the crack tip and resulting in increase of the stresses locally by enhancing the mobility of dislocations. The increase of dislocations on a very local scale because of hydrogen leads to a highly localised fracture, this phenomena is

commonly termed as hydrogen enhanced localised plasticity [16-18]. Thus, the increase of plastic deformation locally at the crack tip can then result in brittle fracture surface appearance, which inherently increases the FCG rate.

4. Conclusions

In the present study, fatigue crack growth resistance of forged Ti-64 was determined in air and gaseous hydrogen environment (15 MPa) at room temperature. The conclusions made from the studies are:

- FCG rate in hydrogen environment remained unaffected at stress intensity ranges below a threshold value i.e. around 20 MPa√m. However it was fluctuating at intermediate stress intensity ranges and increased drastically at higher stress intensity ranges.

- Fatigue fracture surfaces in air consisted of fatigue striations. In contrast, fracture surfaces in hydrogen environment consisted of fatigue striations below a threshold value; brittle flat surfaces and secondary cracks at intermediate stress intensities; and highly deformed surfaces with higher amount of secondary cracks at higher stress intensity ranges.

- It has been suggested that the fluctuations in the crack growth rate at intermediate stress intensity factors could be a result of competing effect of crack deceleration because of crack branching and acceleration because of hydrogen, whereas the later prevails at higher stress intensity ranges.

5. References

[1] Boyer R R 1996 *Mater. Sci. Eng.* A **213 (1-2)** 103-114
[2] Peters M, Kumpfert J, Ward C H and Leyens C 2003 *Adv. Eng. Mater.* **5(6)** 419-427
[3] Tal-Gutelmacher E and Eliezer D 2005 *J. Alloys Comp.* **404-406** 621-625
[4] Walter R J and Chandler W T 1969 *Effects of high pressure hydrogen on metals at ambient temperature* Final report R-7780-l Rocketdyne California USA
[5] Gaddam R, Åkerfeldt P, Pederson R and Antti M L 2011 *Proc. of The 12th World Conf. on Titanium, (Beijing)* **3** (Science Press) 1885-1888
[6] Nelson H G, Williams D P and Stein J E 1972 *Metall. Mater. Trans*. B **3(2)** 469-475
[7] Nelson H G 1976 *Metall. Trans.* A **7A** 621-627
[8] Pittinato G F 1969 *Trans. ASM* **62** 410-417
[9] Pittinato G F 1972 *Metall. Mater. Trans.* B **3(1)** 235-243
[10] ASTM E647-08, "Standard test method for measurement of fatigue crack growth rates", ASTM International, West Conshohocken, PA, DOI: 10.1520/E0647-08, www.astm.org.
[11] ASTM E740-03, "Standard practice for fracture testing with surface-crack tension specimens", ASTM International, West Conshohocken, PA, DOI: 10.1520/E0740-03, www.astm.org.
[12] Evans W, Bache M R, McElhone M and Grabowski L 1997 *Int. J. Fatigue* **19(93**) 177-182
[13] Ding Y S, Tsaya L W and Chen C 2009 *Corros. Sci.* **51** 1413-1419
[14] Nelson H G and Williams D P 1973 *Metall. Mater. Trans.* B **4(1)** 364-367
[15] Janssen M, Zuidema J and Wanhill R 2004 *Fracture Mechanics*, 2nd edition (London and Newyork: Spon Press: Taylor & Francis group) 319-320
[16] Shih, D S, Robertson I M and Birnbaum H K 1988 *Acta Mater*. **36(1)** 111-124
[17] Robertson I M 2001 *Eng. Fract. Mech.* **68(6)** 671-692
[18] Birnbaum H K and Sofronis P 1994 *Mater. Sci. Eng*. A **176(1-2)** 191-202

Acknowledgments
The authors kindly acknowledge Graduate School of Space Technology and National Aviation Engineering Research Programme (NFFP) for funding the research work. We would like to acknowledge Dr. Johanne Mouzon for providing the high resolution scanning electron microscopy facilities at Department of Civil, Environmental and Natural Resources Engineering, Division of Sustainable Process Engineering, Luleå University of Technology, Sweden.